PAPER Special Section on Recent Progress in Antennas and Propagation in Conjunction with Main Topics of ISAP2010

Effectiveness of Short-Range MIMO Using Dual-Polarized Antenna

Ken HIRAGA[†a)], ***Member***, **Tomohiro SEKI**[†], **Kentaro NISHIMORI**[††], ***and*** **Kazuhiro UEHARA**[†], ***Senior Members***

SUMMARY Short-range Multiple-Input-Multiple-Output (SR-MIMO) transmission is an effective technique for achieving high-speed and short-range wireless communication. With this technique, however, the optimum aperture size of array antennas grows when the transmission distance is increased. Thus, antenna miniaturization is an important issue in SR-MIMO. In this paper, we clarify the effectiveness of using dual-polarized planar antennas as a means of miniaturizing SR-MIMO array antennas by measurements and analysis of MIMO transmission characteristics. We found that even in SR-MIMO transmission, the use of dual-polarized transmission enables higher channel capacity. Dual-polarized antennas can reduce by two thirds the array area that is needed to obtain the same channel capacity. For a transmission distance of two wavelengths, the use of a dual-polarized antenna improved the channel capacity by 26 bit/s/Hz while maintaining the same number of transmitters and receivers and the same antenna aperture size. Moreover, dual-polarized SR-MIMO has a further benefit when zero-forcing (ZF) reception without transmit beamforming is adopted, i.e., it effectively simplifies hardware configuration because it can reduce spatial correlation even in narrow element spacing. In this work, we confirmed that the application of dual-polarization to SR-MIMO is an effective way to both increase channel capacity and enhance transceiver simplification.

key words: *short-range MIMO, dual-polarization, array antennas, parallel transmission, high-speed transmission*

1. Introduction

Recently, the transmission speed of optical communications is increasing as fiber to the home (FTTH) has been adopted more widely. Higher data transmission rates over 1 Gbit/s are expected for high definition images and video services [1]. Hence, several Gbit/s to 10 Gbit/s transmission is required for future short range wireless communications. Although high signal-to-noise power ratio (SNR) is guaranteed in short range communications, the transmission rate is saturated due to the limitations on modulation scheme level with a limited frequency band. Within this context, the multiple-input-multiple-output (MIMO) technique has been gathering attention because it can increase the wireless transmission rate without expanding the frequency bandwidth through the use of multiple antennas at the transmitter and receiver [2], [3]. The technique has found practical consumer use in high-speed wireless LAN systems above 100 Mbit/s [4].

Short-range MIMO (SR-MIMO) transmission with multiple data streams between array antennas in a line-of-sight (LOS) environment is an effective transmission technique for short-range communication [5], [6], because there is an optimal condition in which the channel capacity is maximized for a short transmission distance [5]. One of the target scenarios in SR-MIMO is high speed transmission through a concrete wall without any cables [7]. Several-wavelength transmission capability is required for this application. However, in SR-MIMO, larger element spacing is required to obtain maximum channel capacity when the transmission distance is several wavelengths [5]; hence the array size is large in this case. Furthermore, when the number of elements is increased to obtain higher transmission capacity, larger array size is necessary. Therefore, antenna size is one of the major issues in SR-MIMO.

It is well known that dual-polarized antennas are effective in miniaturizing array antennas because their elements have the capability of two elements. Moreover, MIMO transmission using orthogonal polarization has been proposed and evaluated to enhance MIMO transmission performance [8], [9], especially in outdoor scenarios [10], [11].

In this paper, we introduce the use of dual-polarization into antennas for SR-MIMO transmission. However, the application effect of polarization multiplexing using a dual-polarized antenna has not been clarified in SR-MIMO. Hence, in this paper we show that, on the basis of a numerical analysis using Method of Moment (MoM) [12] and an experimental evaluation using a MIMO-Orthogonal Frequency Division Multiplexing (OFDM) testbed that can deal with wireless LAN signals of the IEEE802.11n standard [13], [14], dual-polarized SR-MIMO transmission is more effective than vertically-polarized MIMO in improving transmission rate and miniaturizing array antennas. Since it is known that the positional precision of the opposed transmitting and receiving antenna arrays has a negative effect on MIMO channel capacity [15], we also compare the negative effect of displacement between the transmitting and receiving antenna arrays on dual- and vertically-polarized SR-MIMO transmission.

The remainder of this paper is organized as follows. Section 2 introduces the basic concept of SR-MIMO and describes the concept and antenna models of dual-polarized SR-MIMO. The channel capacity is evaluated using MoM in Sect. 3. Section 4 confirms the effectiveness of the transmission schemes in dual-polarized SR-MIMO by making use of actual OFDM signals.

Manuscript received March 8, 2011.
Manuscript revised July 14, 2011.
[†]The authors are with NTT Network Innovation Laboratories, NTT Corporation, Yokosuka-shi, 239-0847 Japan.
[††]The author is with the Faculty of Engineering, Niigata University, Niigata-shi, 950-2181 Japan.
a) E-mail: hiraga.ken@lab.ntt.co.jp
DOI: 10.1587/transcom.E95.B.87

2. Principle of Dual-Polarized SR-MIMO

2.1 Concept of SR-MIMO and Its Issues

Figure 1 shows a comparison between the basic concepts of general MIMO and SR-MIMO [5]. General MIMO transmission shown in Fig. 1(a) can transmit multiple signal streams by utilizing the multipath-rich environment [2]. Basically, however, multiple data streams cannot be transmitted when a multipath environment is not available. Figure 1(b) denotes the basic concept of SR-MIMO discussed in this paper. To achieve full-rank MIMO transmission, SR-MIMO utilizes the length differences among each path between transmitting (Tx) elements and receiving (Rx) elements. The signal streams are transmitted almost directly between opposing transmitting and receiving elements and the transmission lines are formed in parallel when the transmitting and receiving antenna arrays are in very close proximity. Though the transmission is not completely parallel because the signals reach elements other than the directly facing element, low spatial correlation can be achieved between adjacent elements because the signals that reach those elements have different phases and amplitudes depending on the path length differences. Also, for SR-MIMO transmission, high signal-to-noise-ratio (SNR) can be achieved due to the short transmission distance. Thus, high channel capacity can be expected even if there are no multi-path waves. The principle of SR-MIMO operation is described in more detail in [5].

As a SR-MIMO application in the microwave band, we previously proposed a data relay system that can transmit through a concrete wall (Fig. 2(a)) [7]. As another application, over 100 Gbit/s transmission with a download kiosk

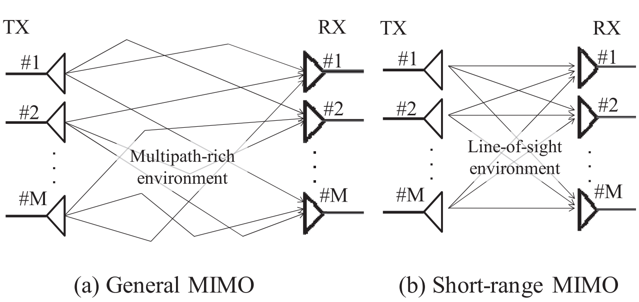

Fig. 1 Basic concept of Short-range MIMO.

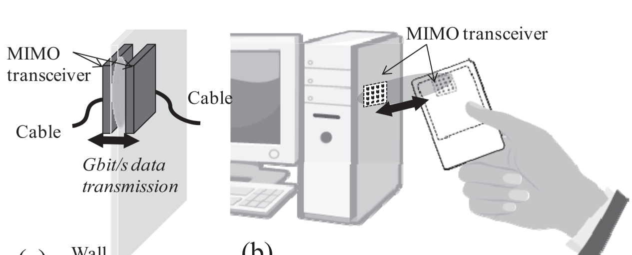

Fig. 2 Target scenario of SR-MIMO.

[16] over a millimeter wave band has been discussed because the band has more frequency resources than a microwave band (Fig. 2(b)) [15].

Figure 3 is the relationship between SR-MIMO channel capacity and antenna element spacing for a four-element square array at the Tx and Rx sides [5]. In the figure, d denotes the element spacing of the Tx and Rx antenna arrays, λ_0 is the free-space wavelength of the RF signal, and D is the transmission distance. As we can see in this figure, element spacing at which maximum channel capacity is obtained, i.e., optimum element spacing, depends on the transmission distance. A transmission distance of several wavelengths between the transmitter and receiver is required for the application shown in Fig. 2(a). However, in SR-MIMO, large element spacing more than $1.0\lambda_0$ is required to obtain maximum channel capacity when the transmission distance is several wavelengths, hence the array size is large in this case. On the basis of this idea, when the number of elements is increased to obtain higher transmission capacity, larger array size is essential. Hence, antenna size is one of the major issues in SR-MIMO.

2.2 Application of Polarization Multiplexing to SR-MIMO

We have proposed SR-MIMO transmission which has employed a single polarized antenna array [15]. On the other hand, dual-polarized antennas are effective in miniaturizing array antennas because their elements have the capability of two elements. In many wireless communication systems, polarization diversity or polarization multiplexing have been studied as techniques to improve frequency utilization [17]. In conventional MIMO transmission utilizing multipath environments, the effect of polarization multiplexing has already been examined [8], [10] and experiments using three orthogonal polarizations have been performed [9], [11]. Up

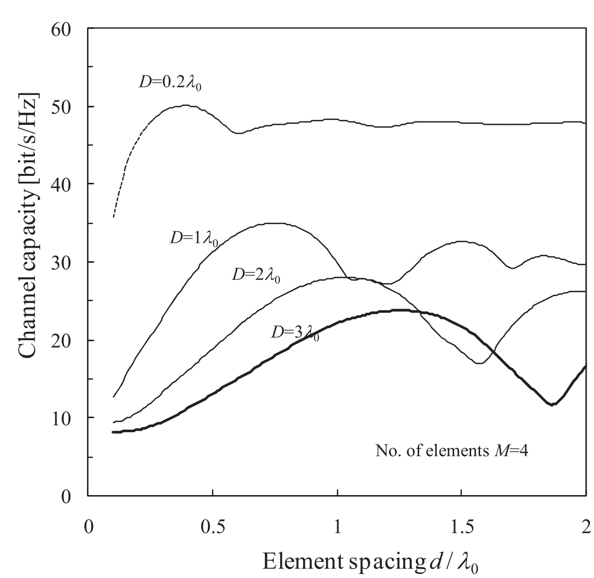

Fig. 3 Optimum element spacing [5].

to now, the application effect of polarization multiplexing using a dual-polarized antenna has not been clarified in SR-MIMO, while an experiment with an array antenna composed of vertically- and horizontally-polarized elements in a MIMO scheme in a line-of-sight (LOS) environment has been reported [18].

In this paper, we introduce dual-polarization to SR-MIMO transmission to achieve antenna miniaturization and its effectiveness is shown throughout the simulations and measurements we performed. In short-range wireless transmission, polarization multiplexing is expected to result in high isolation between paths (i.e., low spatial correlation). This is because there is very little polarization rotation due to reflection and because there is very little polarization rotation when the transmitting and receiving antennas directly face each other. However, in performing SR-MIMO transmission, when dual-polarized elements are arrayed and faced as a transmitting-receiving array, spatial correlation is expected to become higher because there is significant polarization rotation in the path between diagonally-placed elements. In addition, polarization coupling loss stemming from high cross-polarization discrimination (XPD) in the path between directly-faced elements reduces SNR at the MIMO receiver. When XPD is high in SR-MIMO, the spatial correlation is in preferable condition. On the other hand, SNR is not preferable due to the polarization coupling loss. Hence, high XPD is not a simple requirement for this transmission scheme. Since these effects have not been clarified, SR-MIMO transmission characteristics with dual-polarized antenna arrays are clarified in this paper.

2.3 Antenna Configurations for Vertically-/Dual- Polarized SR-MIMO

Figure 4 shows the configurations of the antenna arrays we used in our study. The configuration in Fig. 4(a) is that of an array antenna with vertically-polarized (V-pol) elements for 8×8 SR-MIMO over the 4.85 GHz band. The distance between the TX and RX antenna arrays, i.e., the transmission distance, is D. The elements for both arrays are arranged in the same lattice pattern with element spacing d_V and the number of TX and RX elements M is eight. Each element is a rectangular microstrip antenna 19.6 mm × 19.6 mm in size. The feed point is located 3.10 mm from the center of the microstrip antenna. Electromagnetic simulation by the Method of Moment (MoM) [12] was used to design the elements to have the minimum return loss of −22 dB at 4.85 GHz.

The configuration in Fig. 4(b) is that of an array antenna with dual-polarized (dual-pol) elements for 8×8 SR-MIMO over the 4.85 GHz band. The transmission distance is D. The elements for both arrays are arranged in the same square pattern with element spacing d_{dual}. The elements are dual-polarized microstrip antennas 19.7 mm × 19.7 mm in size. Each element has two feed points, one for V-pol and the other for horizontal-polarization (H-pol). The feed points are located 3.45 mm from the center of the microstrip antenna. The elements are designed to have the minimum return loss of −22 dB at 4.85 GHz. Though this array antenna is for 8×8 SR-MIMO, the number of elements is four because each element has two feed points. Thus, we can decrease the array antenna area by employing the dual-polarized elements.

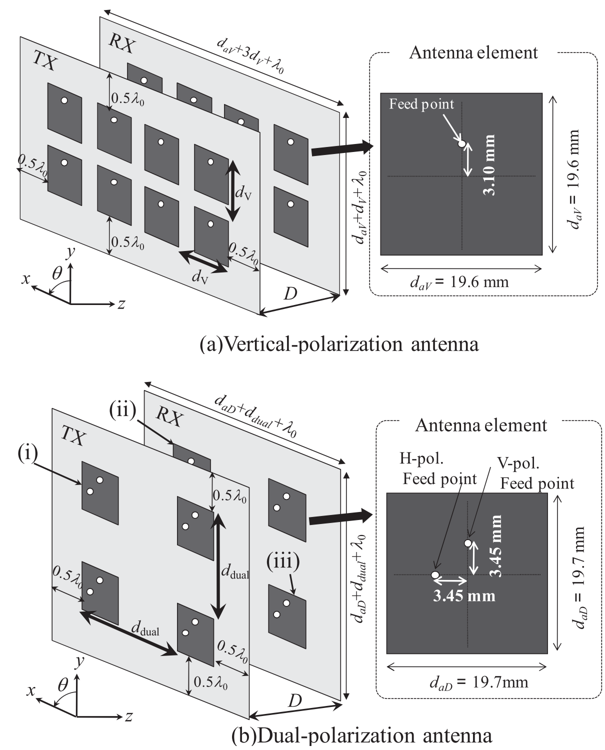

(a)Vertical-polarization antenna

(b)Dual-polarization antenna

Fig. 4 Antenna configurations.

In both models, the arrays are formed on dielectric substrates of a finite size whose thickness is 1.56 mm, the dielectric constant ε_r is 2.17, and the loss tangent tanδ is 0.0008. In both array antennas, there is a margin on the dielectric substrate board in which to form the ground plane of a microstrip antenna. As shown in Fig. 4(a) and Fig. 4(b), the width of this margin is $0.5\lambda_0$. Here, λ_0 is the free-space wavelength of the RF signal. It is not fair to compare the performance of such models having the same element spacing because the geometric arrangement of the dual-pol array antenna is different from that of the V-pol array antenna. Accordingly, we introduce the factor of antenna size ($\sqrt{A}$) defined as: $\sqrt{A} = \sqrt{(d_{aV} + 3d_V + \lambda_0)(d_{aV} + d_V + \lambda_0)}$ for a V-pol array antenna

$\sqrt{A} = \sqrt{(d_{aD} + d_{dual} + \lambda_0)^2} = d_{aD} + d_{dual} + \lambda_0$ for a dual-pol array antenna.

Here, d_{aV} is the width or length of V-pol antenna elements, and d_{aD} is the width or length of dual-pol antenna elements. Hence, A is equal to the area of the array antenna.

3. Effectiveness of Dual-Polarized SR-MIMO; Basic Characteristics Analysis

Simulation was performed at 4.85 GHz (Bandwidth is 20 MHz) using MoM [12] for consistency with the measurement results in Sect. 4. The S-parameters are then converted to the channel matrix.

In this section, channel capacity and XPD with dual-polarized antenna arrays are clarified. Here, channel capacity C is calculated using the equation below.

$$C = \log_2 \det\left(\mathbf{I} + \frac{P_s}{\sigma^2 M}\mathbf{H}\mathbf{H}^H\right) \tag{1}$$

Here, **I** and **H** denote the unit matrix ($M \times M$ matrix, M: the number of antenna elements) and the channel matrix, respectively, P_s is total transmission power at the transmitter, and σ^2 is noise power at the receiver side. Assuming the same transmitting power at each element, maximum channel capacity is calculated by using Eq. (1) when the channel information is unknown by the transmitter [19], [20]. The transmission characteristics between the transmitting and receiving elements are calculated as S-parameters by MoM, as described below.

The channel capacity is calculated from the transmission characteristics by using Eq. (1). In this analysis, the distance between the transmitting (Tx) and receiving (Rx) antenna arrays is D. Models for electromagnetic simulation are composed as shown in Fig. 4(a) and Fig. 4(b). The electromagnetic simulation includes the effects of the coupling between Tx and Rx elements, the effects of the mutual coupling between elements in the same array, and the effects of the edge of the dielectric substrate. The ratio of P_s to σ^2 is 49 dB.

Figure 5(a) shows the calculated XPDs (antenna size $\sqrt{A}/\lambda_0$ is 1.3) at the paths from element (i) to element (ii) and from element (i) to element (iii). The XPD at the path between directly facing elements, i.e., the path from (i) to (ii), is more than 23 dB. On the other hand, it is less than 10 dB at the path between diagonally-located elements when the transmission distance D is less than 80 mm. In the diagonal path, RF signals transmitted at the V-pol feed point can be received at the H-pol feed point of the receiver's element. This is inconvenient in conventional polarization multiplexing. However, if spatial correlation is sufficiently low in each path, spatial division multiplexing is achievable under low XPD because we assume MIMO is the multi-stream transmission scheme.

We investigated the transmission characteristics of each polarization path. Figure 5(b) shows the phase difference between path #1 and path #2, whose details are shown in Table 1. Though these paths are nearly equal in length and geometric shape, they have rather different phase characteristics as shown in the figure. Similar results are obtained when the relation between the V-pol. and H-pol. feed points is the opposite from that in this case (not shown in the figure). When either phase difference or high XPD is maintained, dual-polarized SR-MIMO is expected to have high channel capacity.

Figure 6(a) compares the channel capacity versus antenna size for dual-pol and V-pol. As the figure shows, when D = 120 mm, the channel capacity is 76 bit/s/Hz at $\sqrt{A}/\lambda_0$ = 1.6 and at $\sqrt{A}/\lambda_0$ = 1.3 for vertical and dual

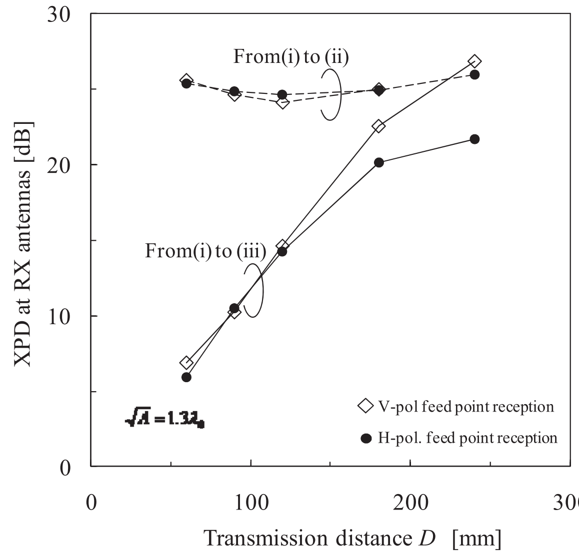

(a) XPD

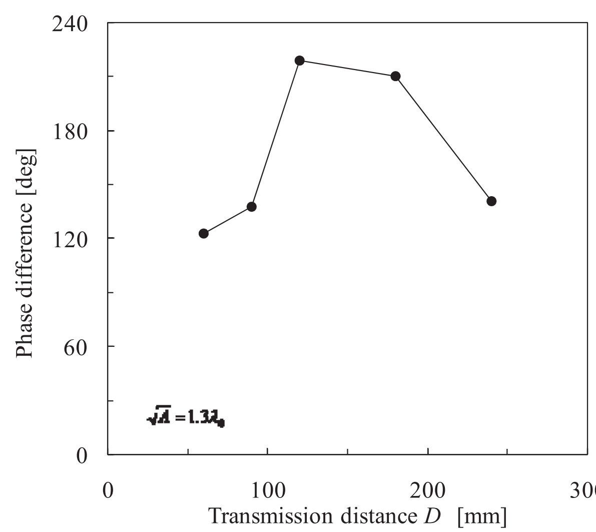

(b) Phase difference between path #1 and path #2

Fig. 5 Polarization characteristics (simulation).

Table 1 Paths between elements (i) and (iii).

Path no.	Tx feed point in (i)	Rx feed point in (iii)
1	V-pol feed point	H-pol feed point
2	H-pol feed point	H-pol feed point

polarizations, respectively. At this time antenna area is reduced from $(1.6\lambda_0)^2$ to $(1.3\lambda_0)^2$ when the channel capacity is 63 bit/s/Hz. In other words, antenna size is reduced by two thirds using dual polarizations.

Hence, the dual-polarized SR-MIMO transmission can reduce antenna size. In addition, significant channel capacity improvement is observed with the same antenna size. For example, when D=120 mm and $\sqrt{A}/\lambda_0$ = 0.95, channel capacity is increased from 40 bit/s/Hz to 66 bit/s/Hz by em-

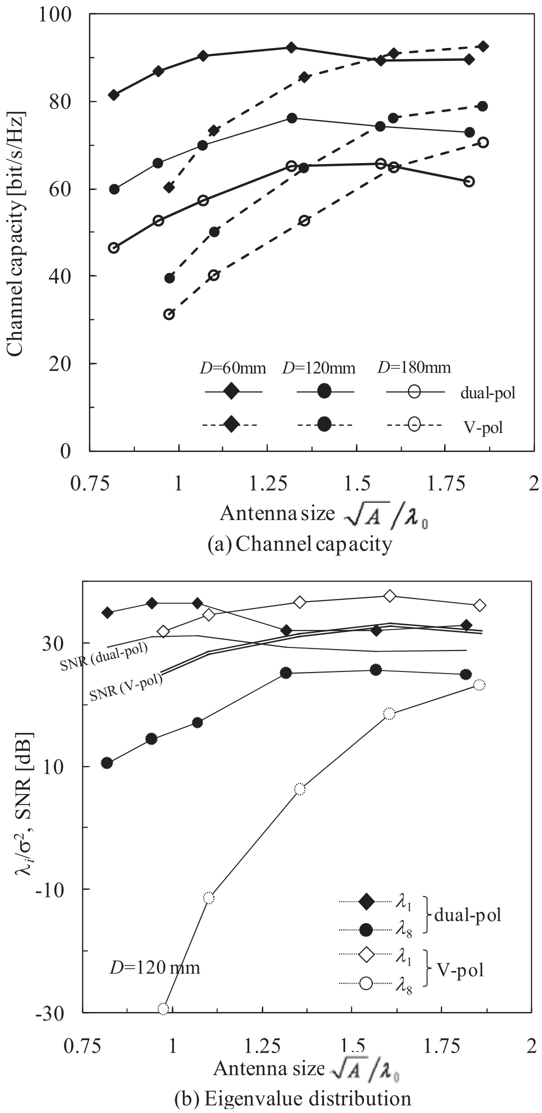

(a) Channel capacity

(b) Eigenvalue distribution

Fig. 6 Antenna size $\sqrt{A}$ comparisons. (simulation)

ploying a dual-pol antenna. This means that we can increase channel capacity with the same equipment complexity and the same antenna array area by applying the dual-polarized SR-MIMO transmission.

Figure 6(b) compares 1st and 8th eigenvalues and SNR versus the antenna size for the dual-pol and V-pol SR-MIMO when the transmission distance D is 120 mm. The eigenvalues shown in Fig. 6 are the ratio of actual eigenvalue to noise power. The SNR shown in the figure is the average of all eigenvalues. As can be seen, the difference between the 1st and 8th eigenvalues (λ_1 and λ_8 in the figure) for dual-pol is smaller than that for V-pol, especially when the antenna size is small. Hence, dual-pol uses data streams that correspond to minor eigenvalues for data transmission. This enables improvement in the channel capacity. Since antenna size becomes larger as transmission distance becomes longer, dual-pol antennas are expected to be particularly useful in reducing array area size when the transmission distance is long.

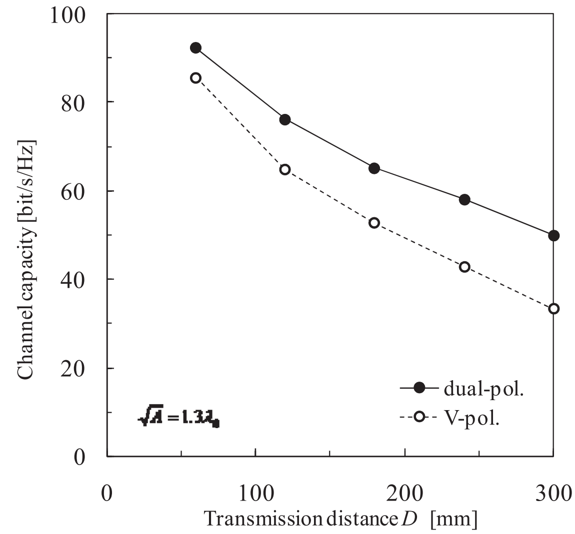

Fig. 7 Channel capacity vs. transmission distance. (simulation)

Figure 7 compares dual-pol and V-pol in terms of the relationship between channel capacity and transmission distance D when the antenna size $\sqrt{A}/\lambda_0$ is 1.3. We can see that the effect of dual-pol becomes larger as D increases. When D = 60 mm, channel capacity is higher than that of D = 120 mm, though XPD decreases significantly as D decreases as Fig. 5(a) shows. We can see that XPD is around 5 dB when D = 60 mm (see "From (i) to (iii)" in Fig. 5(a)), and 15 dB when D = 120 mm. On the other hand, the phase difference is as many as 120 degrees when D = 60 mm. Note that unlike in conventional polarization multiplexing, low XPD is preferable in SR-MIMO in cases where there is a phase difference in paths, because received cross-polarized RF signals are utilized for demodulation at the receiver.

4. Evaluation of Frequency Utilization Using MIMO Testbed and Measured Channels

This section details experiments we performed to verify that the simulation models mentioned above are appropriate for evaluating SR-MIMO characteristics. We clarify the effectiveness of dual-polarized SR-MIMO transmission by using actual OFDM signals stipulated in the IEEE802.11n standard. Also clarified is the negative effect of displacement between the transmitting and receiving antenna arrays on SR-MIMO transmission performance. Here, simulated values that are described as "MoM" in Figs. 9–12 and 14 in later sections are calculated from the simulated S-parameters shown in Sect. 3 using actual OFDM signal transmission simulations [13].

In the analyses and measurements shown in this section, the ratio of total transmission power and noise power at the receiver is 49 dB. This condition is the same as that applied in the analyses described in Sect 3.

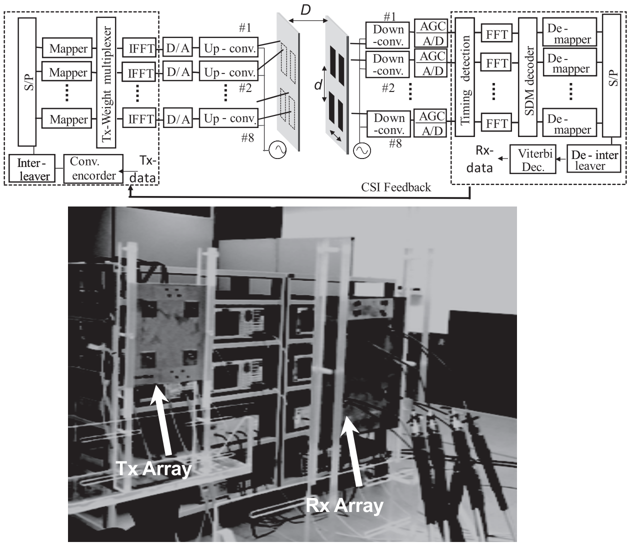

Fig. 8 MIMO testbed for the measurement.

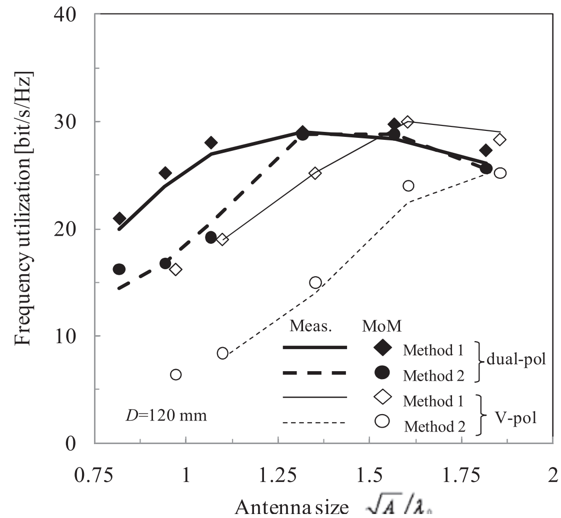

Fig. 9 Frequency utilization versus antenna size.

Table 2 Measurement parameters.

Center frequency	4.85 GHz
No. of antennas	8 (Tx, Rx)
Transmit signal level	-25 dBm
Bandwidth	20 MHz
FFT points	64
No. of subcarriers	53
Modulation scheme	QPSK～1024QAM
Coding rate	1/2, 2/3, 3/4, 5/6, 7/8

4.1 Measurement Setup

To verify the results of the numerical analysis we had obtained, we carried out measurements using a MIMO testbed [14]. Figure 8 shows the MIMO testbed used in the measurements. Using this testbed, 8×8 MIMO channels were measured. The measurement parameters are shown in Table 2. The frequency and bandwidth were 4.85 GHz and 20 MHz, respectively. Array antennas were fabricated with the configuration described in Sect. 2.3. We used actual signals of the type specified in the IEEE 802.11n standard [4], because MIMO techniques had already been established in this standard.

The MIMO testbed we used is capable of handling high modulation schemes such as 256 QAM and 1024 QAM with the coding rate of 7/8, because this testbed was built for multi-user MIMO transmission that requires a higher total transmission bit rate than that of single-user MIMO. In SR-MIMO evaluation, it is possible to evaluate very high transmission rates, i.e., over 1 Gbps. Further details of the testbed are described in [14]. The testbed supports adaptive modulation schemes that respond to the eigenvalue, which is obtained by the channel state information (CSI) between the transmitter and the receiver. We used the table described in [14] to select the modulation scheme and coding rate.

In this experiment, transmission performance is evaluated with two transmission methods; one employs eigenmode beamforming (EM-BF) at the transmitter and the other employs no beamforming. Each scheme adopts zero forcing (ZF) decoding.

(Method 1)
Tx: Eigenmode beamforming (EM-BF),
Rx: Zero Forcing (ZF)
(Method 2)
Tx: Without beamforming,
Rx: ZF

4.2 Evaluation by Frequency Utilization

Figure 9 shows the measured frequency utilization obtained for dual-pol and V-pol with transmission methods 1 and 2, respectively. Figure 10 shows the eigenvalue distribution versus antenna size. Here, the transmission distance D is 120 mm. Note that the frequency utilization is completely different from the channel capacity. Although the channel capacity is expressed by using Eq. (1) in Sect. 3, the frequency utilization is an actual transmission rate per Hz when considering the PHY layer of the IEEE802.11n standard; the actual rate is frequency utilization $\times$ 20 MHz in this measurement. Since the measured frequency utilization well matches that obtained from simulation, the simulation models are considered to be valid for the evaluation of dual-polarized SR-MIMO performance.

As shown in Fig. 9, in V-pol SR-MIMO, the frequency utilization of transmission method 2 is much lower than that of method 1. On the other hand, in dual-pol SR-MIMO, the frequency utilization of transmission method 1 is improved and the difference between the two methods is smaller than in V-pol SR-MIMO, because the performance is degraded by ZF without transmission beamforming when the spatial correlation is high or the ratio between the 1st and other

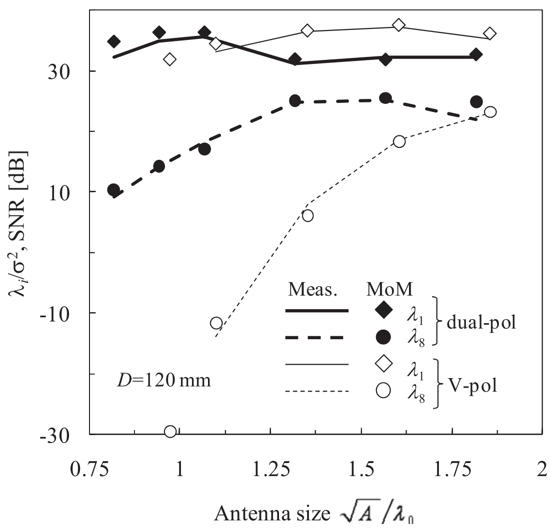

Fig. 10 1st and 8th eigenvalues.

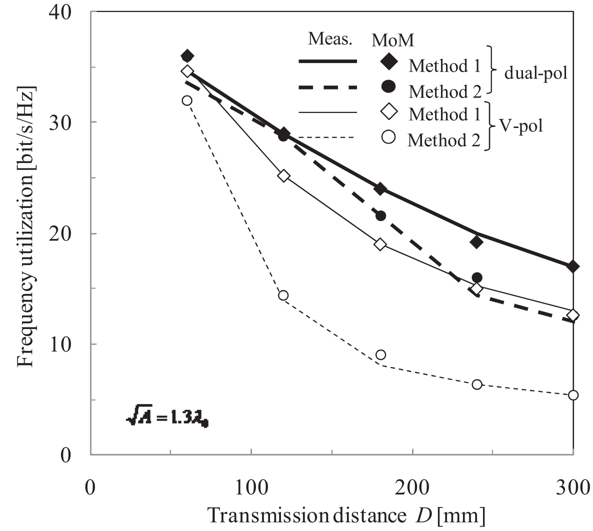

Fig. 12 Frequency utilization versus transmission distance.

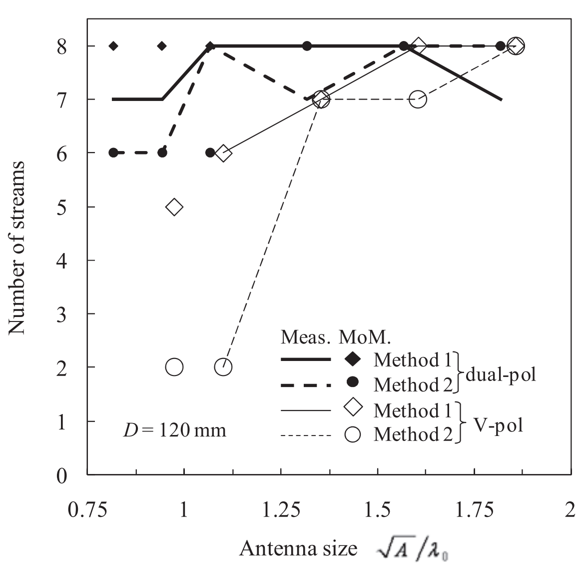

Fig. 11 Number of streams with maximum frequency utilization without error.

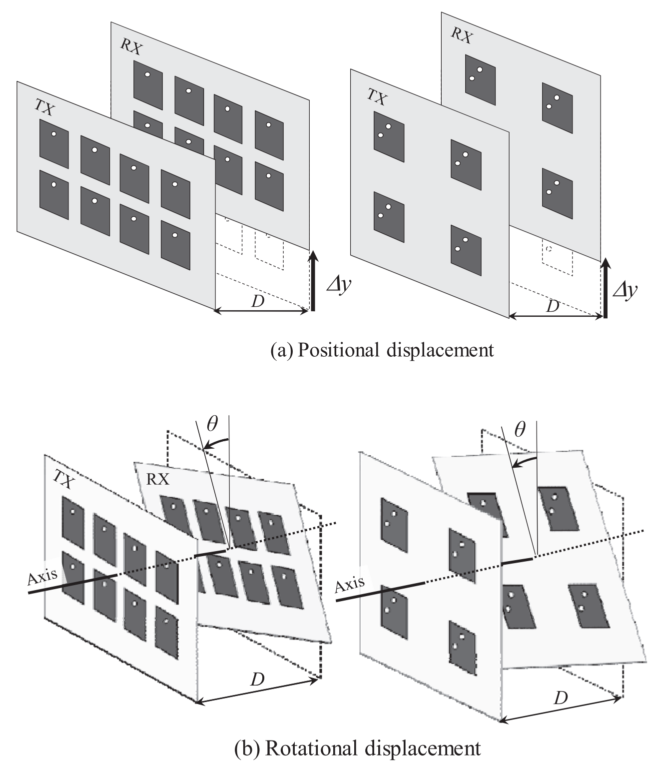

Fig. 13 Antenna displacement types.

eigenvalues is large. Thus dual-pol is particularly useful when transmission beamforming is not performed. In performing MIMO transmission using only ZF reception, complex operations such as singular value decomposition (SVD) or CSI feedback are not needed. In other words, dual-pol reduces signal processing cost and hardware configuration complexity.

As can be seen in Fig. 10, the 8th eigenvalue is significantly improved by applying dual-pol. This contributes to improved transmission speed performance. Again, the measured results well match the simulated ones. Figure 11 shows the number of streams with maximum frequency utilization with error-free transmission. It is clear that more data streams are available when dual-pol is applied, especially in ZF with $\sqrt{A}/\lambda_0 < 1.3$.

Figure 12 shows measured frequency utilization versus transmission distance. The antenna size $\sqrt{A}/\lambda_0$ is 1.3 here. As the figure shows, frequency utilizations of method 1 have decreasing characteristics as D increases that are similar to the channel capacity shown in Fig. 7. For example, when D=120 mm, performance improvements by applying dual-pol are 15.0 bit/s/Hz without beamforming and 3.8 bit/s/Hz with beamforming. Throughout the transmission distance, the improvement is larger without than with transmission beamforming. It is clear that the application of dual-pol on SR-MIMO is effective in improving frequency utilization

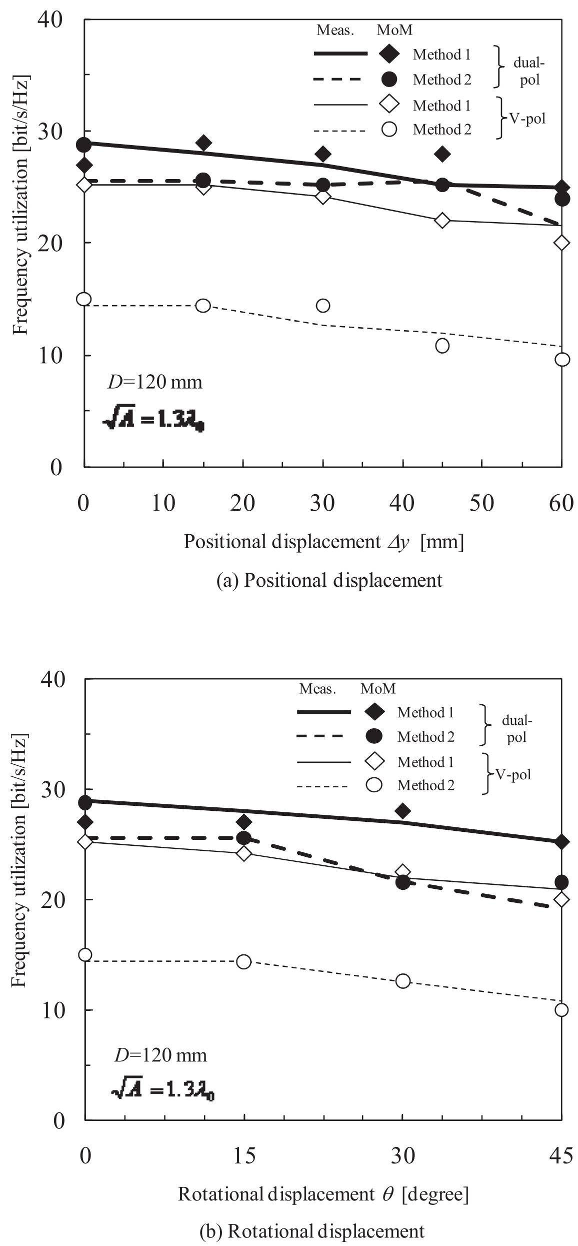

Fig. 14 Effect of antenna array displacement.

performance.

4.3 Negative Effect of Antenna Displacement

Since it is known that the positional precision of the opposed transmitting and receiving antenna arrays has a negative effect on channel capacity [15], the negative effects of displacement between the transmitting and receiving antenna arrays on dual- and vertically-polarized SR-MIMO transmission have to be clarified. We measured and analyzed the effect of positional precision of the antenna.

Figure 13(a) shows antenna arrays with positional displacement Δy and (b) shows arrays with rotational displacement θ.

Figure 14 compares measured and simulated results. The simulation was performed under the same conditions as described above. We can see that the degree of performance deterioration caused by displacement is similar for both V-pol and dual-pol. The simulated and measured results show good agreement.

5. Conclusion

The transmission characteristics and mechanism of dual-polarized SR-MIMO were investigated by simulations and measurements. Although SR-MIMO usually utilizes the length differences among each path between transmitting elements and receiving elements, channel capacity is maintained because there are phase differences between cross-polarized paths which have very similar geometric ray paths. The use of a dual-polarized (dual-pol) antenna can reduce the array area size by two thirds while maintaining the same transmission performance. It also significantly improves channel capacity with the same antenna size and equipment complexity. For example, when the antenna size is $0.95\lambda_0$, channel capacity is increased from 40 to 66 bit/s/Hz with the use of a dual-pol antenna. This means that using such an antenna can increase channel capacity with the same equipment complexity and the same antenna array area.

In an experiment using a MIMO-OFDM testbed, dual-pol SR-MIMO was found to have another advantage when zero-forcing (ZF) reception without transmission beamforming is adopted, i.e., it enables hardware configuration to be simplified. Because measured and simulated eigenvalue distributions showed good agreement, we believe that the simulation we performed is valid for purposes of evaluation.

We also measured SR-MIMO performance degradation caused by antenna array displacement and found that the degree of performance deterioration caused by displacement is similar for both vertical polarization and dual polarization.

Our conclusion is that applying dual-polarization to SR-MIMO effectively improves transmission performance, facilitates transceiver simplification, and enhances array antenna miniaturization.

Acknowledgements

The authors would like to thank Associate Professor Dr. Naoki Honma at Iwate University for his insightful comments and suggestions on SR-MIMO technique. They also appreciate the helpful support in experiments and analyses provided by Mr. Yuki Onuma and Mr. Ryouchi Kataoka at the Faculty of Engineering, Niigata University.

References

[1] B. Bosco, R. Emrick, J. Holmes, R. Lempkowski, and S. Rockwell, “Gigabit wireless personal area networks: Motivation, challenges and implementation,” IEEE Radio and Wireless Symposium, 2009. (RWS’09.), pp.574–577, 2009.

[2] D. Gesbert, M. Shafi, Da-shan Shiu, P.J. Smith, and A. Naguib,

"From theory to practice: An overview of MIMO space-time coded wireless systems," IEEE J. Sel. Areas Commun., vol.21, no.3, pp.281–302, April 2003.
[3] M.A. Jensen and J.W. Wallace, "A review of antennas and propagation for MIMO wireless communications," IEEE Trans. Antennas Propag., vol.52, no.11, pp.2810–2824, Nov. 2004.
[4] IEEE Std. 802.11n. [Online]. http://www.ieee802.org/11/
[5] N. Honma, K. Nishimori, T. Seki, and M. Mizoguchi, "Short range MIMO communication," 3rd European Conference on Antennas and Propagation (EuCAP 2009), March 2009.
[6] I. Sarris and A.R. Nix, "Design and performance assessment of high-capacity MIMO architectures in the presence of a line-of-sight component," IEEE Trans. Veh. Technol., vol.56, no.4, pp.2194–2202, July 2007.
[7] T. Seki, K. Nishimori, K. Hiraga, and K. Nishikawa, "High speed parallel data transmission technology for short range wireless relay system," IEICE Technical Report, AP2009-55, July 2009.
[8] J.P. Kermoal, L. Schumacher, F. Frederiksen, and P.E. Mogensen, "Experimental investigation of the joint spatial and polarisation diversity for MIMO radio channel," Wireless Personal Multimedia Communication 2001, Sept. 2001.
[9] N.K. Das, T. Inoue, T. Taniguchi, and Y. Karasawa, "An experiment on MIMO system having three orthogonal polarization diversity branches in multipath-rich environment," IEEE 60th Vehicular Technology Conference, p.1528, 2004.
[10] V. Eiceg, H. Sampath, and S. Catreux-Erceg, "Dual-polarization versus single-polarization MIMO channel measurement results and modeling," IEEE Trans. Wirel. Commun., vol.5, no.1, pp.28–33, Jan. 2006.
[11] M.C. Mtumbuka and D.J. Edwards, "Experimental investigation of a joint dual-spaced diversity and tri-polarised MIMO system for beyond 3G," Fifth IEE International Conference on 3G Mobile Communication Technologies, 2004, p.373, 2004.
[12] Mentor Graphics. The IE3D™electromagnetic design. [Online]. http://www.mentor.com/electromagnetic-simulation/
[13] K. Nishimori, N. Honma, T. Seki, and K. Hiraga, "On the transmission method for short range MIMO communication," IEEE Trans. Veh. Technol., accepted.
[14] K. Nishimori, R. Kudo, N. Honma, Y. Takatori, and M. Mizoguchi, "16×16 MIMO testbed for MU-MIMO downlink transmission," IEICE Trans. Commun., vol.E93-B, no.2, pp.345–352, Feb. 2010.
[15] K. Hiraga, T. Seki, K. Nishimori, K. Nishikawa, and K. Uehara, "Ultra-high-speed transmission over millimeter-wave using microstrip antenna array," 2010 IEEE Radio and Wireless Symposium (RWS), New Orleans, LA, p.673, 2010.
[16] A. Sadri, (2006, Nov.) Summary of the Usage models for 802.15.3c. [Online]. http://www.ieee802.org/15/pub/TG3c.html
[17] W. Lee and Y. Yeh, "Polarization diversity system for mobile radio," IEEE Trans. Commun., vol.20, no.5, pp.912–923, Oct. 1972.
[18] T. Mizuno, S. Kojima, K. Nakamura, K. Yoshitomi, K. Asanuma, and T. Maeda, "The effects of antenna arrangement and human hand on the MIMO channels for short range wireless communication," IEICE Technical Report, AP2007-180, March 2008.
[19] T. Ohgane, T. Nishimura, and Y. Ogawa, "Applications of space division multiplexing and those performance in a MIMO channel," IEICE Trans. Commun., vol.E88-B, no.5, pp.1843–1851, May 2005.
[20] G.J. Foschini and M.J. Gans, "On limits of wireless communications in a fading environment when using multiple antennas," Wirel. Pers. Commun., vol.6, no.3, pp.311–335, March 1998.

Ken Hiraga received the B.E. and M.E. degrees in electronics and information engineering from Hokkaido University, Sapporo, in 2003 and 2005 respectively. Since 2005, he has been engaged in research and development on cognitive radio systems and high-speed wireless systems at Nippon Telegraph and Telephone Corporation (NTT). He received the Young Engineers Award from the IEICE in 2010. He is currently working towards his Ph.D. in Hokkaido University. He is a member of IEEE.

Tomohiro Seki received his B.E., M.E. and Dr. Eng. degrees in electrical engineering from the Tokyo University of Science, Tokyo, Japan, in 1991, 1993 and 2006, respectively. In 1993, he joined NTT and has been engaged in research on planar antennas and active integrated antennas for the millimeter-wave and microwave bands. He is currently interested in system-on-package technologies for millimeter-wave communication systems. He is a senior research engineer of NTT Network Innovation Laboratories. He received the 1999 Young Engineer Award presented by the IEICE and the 2006 Best Paper Award presented by IEICE Communications Society. He is a member of IEEE.

Kentaro Nishimori received the B.E., M.E. and Ph.D. degrees in electrical and computer engineering form Nagoya Institute of Technology, Nagoya, Japan in 1994, 1996 and 2003, respectively. In 1996, he joined the NTT Wireless Systems Laboratories, Nippon Telegraph and Telephone Corporation (NTT), in Japan. He was senior research engineer on NTT Network Innovation Laboratories. He is now associate professor in Niigata University. He was a visiting researcher at the Center for Teleinfrastructure (CTIF), Aalborg University, Aalborg, Denmark from Feb. 2006 to Jan. 2007. He was an Associate Editor for the Transactions on Communications for the IEICE Communications Society from May 2007 to May 2010 and Assistant Secretary of Technical Committee on Antennas and Propagation of IEICE from June 2008 to May 2010. He received the Young Engineers Award from the IEICE of Japan in 2001, Young Engineer Award from IEEE AP-S Japan Chapter in 2001, Best Paper Award of Software Radio Society in 2007 and Distinguished Service Award from the IEICE Communications Society in 2005, 2008 and 2010. His main interests are spatial signal processing including MIMO systems and interference management techniques in heterogeneous networks. He is a member of IEEE.

Kazuhiro Uehara Senior Research Engineer, Supervisor, Group Leader, Wireless Systems Innovation Laboratory, NTT Network Innovation Laboratories. He received the B.E., M.E., and Ph.D. degrees from Tohoku University, Miyagi, in 1987, 1989, and 1992, respectively. In 1992, he joined NTT and engaged in the research on of array antennas, active antennas, and indoor propagation in the millimeter-wave and microwave frequency bands. From 1997 to 1998, he was a Visiting Associate at the Department of Electrical Engineering, California Institute of Technology, USACA. From 2003 to 2010, he was a part-time lecturer at the Department of Electrical Engineering, Tohoku University. His current interests include the R&D of software defined radio and cognitive radio systems and millimeter-wave multi-gigabit wireless systems. From 2009 to 2011, he was Chair of the Technical Committee on Software Radio, IEICE Communication Society. He was a General Co-Chair of the 6th International Conference on Cognitive Radio Oriented Wireless Networks and Communications, CrownCom, June 2011. He is a Guest Editor-in-Chief of the Special Section on Wireless Distributed Networks, and the Special Section on Cognitive Radio and Heterogeneous Wireless Networks in Conjunction with Main Topics of CrownCom2011, IEICE Transactions on Communications, December 2010 and April 2012, respectively. From 2011, he is a Councilor of Tokyo Section, IEICE. He received the Young Researcher's Award, the Best Paper Award, the Communications Society Outstanding Contributions Award, and the Communications Society Distinguished Contributions Award from IEICE in 1995, 1997, and twice in 2011, respectively, the 1st YRP Award in 2002, and the 18th Telecom System Technology Award from the Telecommunications Advancement Foundation in 1995, 1997, 2002, and 2003, respectively. He is a senior member of IEEE.